Phase Equilibria in the Ln_2O_3-V_2O_3-V_2O_5 (Ln=Pr, Tb, and Y) Systems at 1200 °C

Kenzo Kitayama* and Takashi Katsura
Department of Chemistry, Faculty of Science, Tokyo Institute of Technology,
Ookayama, Meguro-ku, Tokyo 152

(Received July 27, 1984)

The phase equilibria in the systems, Pr_2O_3-V_2O_3-V_2O_5, Tb_2O_3-V_2O_3-V_2O_5, and Y_2O_3-V_2O_3-V_2O_5, were established at 1200 °C by changing the oxygen partial pressure from −1.20 (in the CO_2) to 7.50 in $-\log(P_{O_2}/\mathrm{Pa})$ for Pr_2O_3 and Tb_2O_3 systems, and from −4.32 (in the air) to 7.50 in $-\log(P_{O_2}/\mathrm{Pa})$ for Y_2O_3 system. In the first system $0.81Pr_2O_3\cdot0.19V_2O_5$ (A) and $3Pr_2O_3\cdot V_2O_5$ (B), in the second $0.81Tb_2O_3\cdot0.19V_2O_5$ (A′), and in the last one $4Y_2O_3\cdot V_2O_5$ (A″) were stable in addition to Ln_2O_3, $LnVO_4$, $LnVO_3$, V_nO_{2n-1} (n= 2—7, and Ln means Pr, Tb, and Y), and VO_2 under the present experimental conditions. On the basis of the established phase diagrams, the standard Gibbs energies (ΔG°) of reactions appeared in the systems were calculated. Compounds A, B, $PrVO_3$, A′, A″, and $LnVO_4$ have nonstoichiometric compositions. ΔG° values for the reactions and crystallographic values of the compounds were represented as a function of the ionic radius of lanthanoid (including Y) elements.

Phase equilibria in the Ln_2O_3-V_2O_3-V_2O_5 systems (Ln=Sm, Lu, Er, Gd, La, Nd, Tm, Eu, Yb, Dy, and Ho) at 1200 °C have been established[1-9] by changing the oxygen partial pressure from −4.32 to 7.50 or 9.00 in terms of $-\log(P_{O_2}/\mathrm{Pa})$. The standard Gibbs energy of the reactions appeared in the established systems and the crystallographic data of the ternary compounds and the activities of the components in the solid solutions were also successfully obtained.

In the present study, Pr_2O_3, Tb_2O_3, and Y_2O_3 were chosen as Ln_2O_3. It was well known that Pr_2O_3 and Tb_2O_3 were unstable in air. They change compositions to Pr_6O_{11} and Tb_4O_7 or other compositions depending upon the oxygen partial pressure and the temperature.[10-14] Recently, the oxygen partial pressure ranges in which Pr_2O_3 and Tb_2O_3 are stable have been determined at 1000°, 1100°, and 1200 °C by Sugihara.[15] According to his results, Pr_2O_3 is stable in the $\log P_{O_2}$ range from 4.30 to −11.00 and Tb_2O_3 in the $\log P_{O_2}$ range from 3.25 to −11.00 at 1200 °C. Thus the oxygen partial-pressure range in the present experiments was confined to pressures lower than $10^{1.20}$ Pa (in the CO_2) for both systems. On the other hand, Y_2O_3 is stable in air and, thus, the experimental atmosphere was extended to an air atmosphere from a CO_2 atmosphere.

Livin[16] studied Y_2O_3-V_2O_5 in the temperature range from 650° to 1800 °C and found three compounds $4Y_2O_3\cdot V_2O_5$, $5Y_2O_3\cdot V_2O_5$, and YVO_4 with a melting point 1810±25 °C. He also pointed out that the Y_2O_3-YVO_4 subsystem is probably pseudo-binary because of oxygen losses from the 4:1 and 5:1 phases. Brusset *et al.*[17] studied three systems, Pr_2O_3-V_2O_5, Tb_2O_3-V_2O_5, and Y_2O_3-V_2O_5, in the temperature range from 600° to 1500 °C. $4Pr_2O_3\cdot V_2O_5$, $6Pr_2O_3\cdot V_2O_5$, $4Tb_2O_3\cdot V_2O_3$, $5Tb_2O_3\cdot V_2O_5$, $4Y_2O_3\cdot V_2O_5$, and $5Y_2O_3\cdot V_2O_5$ were found in addition to $LnVO_4$.

In the Pr_2O_3-V_2O_3, Tb_2O_3-V_2O_3, and Y_2O_3-V_2O_3[18] systems, $PrVO_3$, $TbVO_3$, and YVO_3 were well known, but these systems have not yet been completely studied, because V_2O_3 is unstable in the air. The crystallographic properties of these $LnVO_3$ have been investigated by McCarthy *et al.*[19] and Shin-ike *et al.*[20] and it has been confirmed that these compounds are orthorhombic.

The objectives of the present experiments were: (1) to establish the detailed phase equilibria in the systems at 1200 °C in order to confirm which compounds are stable under the present experimental conditions, (2) to calculate the standard Gibbs energies of reactions which appear in the established phase diagrams, and (3) to examine the fitness of the present data on the linear relationship between ΔG° values for the reaction, $LnVO_3+1/2\ O_2=LnVO_4$ and the ionic radius of the lanthanoid elements, including Y.

Experimental

Pr_2O_3, Tb_2O_3, and Y_2O_3 (99.9%), V_2O_5 were used as starting materials. V_2O_5 was prepared by heating a guaranteed grade of NH_4VO_3 at 500 °C in air for about 24 h. Pr_2O_3 and Tb_2O_3 were prepared by reducing the commercial Pr_6O_{11} (99.9%) and Tb_4O_7 (99.9%) in an atmosphere of $\log(P_{O_2}/\mathrm{Pa})=-5.00$ at 1200 °C for about 5 h. The hexagonal, light-green Pr_2O_3 and white Tb_2O_3 with C-form were confirmed by the powder X-ray diffraction method[21,22] and the compositions were determined to be $Pr_2O_{3.00}$ and $Tb_2O_{3.00}$ by EDTA titration. Desired Pr_2O_3/V_2O_5, Tb_2O_3/V_2O_5, and Y_2O_3/V_2O_5 mole ratios of samples were obtained by thoroughly mixing appropriate quantities in an agate mortar under ethyl alcohol. The mixtures, thus obtained, were treated by the same procedures in the previous paper.[1] The apparatus and procedures for controlling the oxygen partial pressure and keeping a constant temperature, the method of thermogravimetry, the criterion for an equilibrium establishment, and the method of the chemical analysis for the mixtures of Y_2O_3 and V_2O_5 were the same as those described in previous reports.[1,23-27] The vanadium content of the mixtures of V and Pr and of V and Tb was volumetrically determined after confirming that the consumption of the $KMnO_4$ standard solution by the coexisting Pr and Tb was within the experimental errors. Samples used for analysis were prepared in the atmosphere, in which the stoichiometric V_2O_3, $LnVO_3$, and Ln_2O_3 were stable at 1200 °C. Pr_2O_3 and Tb_2O_3 contents were determined as a difference between the V_2O_3 weight and the total weight.

Results and Discussion

Phase Equilibria. Nine samples with Pr_2O_3/V_2O_5 mole ratios of 85/15, 8/2, 77/23, 7/3, 65/35, 1, 4/6, 3/7, and 15/85 were prepared to be used in the thermogravimetric experiments. In Figs. 1a and 1b the relationships between the oxygen partial pressure, $-\log(P_{O_2}/\mathrm{Pa})$, on the ordinate and the weight change, W_{O_2}/W_T, on the abscissa are shown as representative cases with four samples, 85/15, 77/23, 65/35, and 15/85. Here, W_{O_2} is the weight gain of the samples from the reference weight in an atmosphere of $\log P_{O_2}=-7.50$, and W_T is the calculated total weight increase of samples which might be obtainable if V_2O_3 in the samples at the reference state would change to V_2O_5 in the higher oxygen pressures. The W_{O_2}/W_T ratio was usually shown in the range from 0.995 to 1.00. From Fig. 1 the oxygen partial pressure in equilibrium 6.75, 4.56, 4.14, and 4.02 in $-\log P_{O_2}$ were found in addition to those in the V_2O_3-VO_2 subsystem.[1]

The identification of the phases was performed with the quenched samples using a powder X-ray diffractometer with Cu *Kα* radiation. The following phases and two-phase combinations are present under the present experimental conditions: $0.81Pr_2O_3\cdot0.19V_2O_5$(A), $3Pr_2O_3\cdot V_2O_5$(B), Pr_2O_3(R), $PrVO_4$(T), $PrVO_3$(O), and VO_2(J) in addition to six compounds in the V_2O_3-VO_2 system,[1] and Pr_2O_3+A,A+B,B+$PrVO_4$, Pr_2O_3+$PrVO_3$, A+$PrVO_3$, B+$PrVO_3$, V_2O_3+$PrVO_3$, V_2O_3+$PrVO_4$, $V_nO_{2n-1}(n=2-7)$+$PrVO_4$, and VO_2+$PrVO_4$.

Based upon the above experimental results from the thermogravimetry and the identification of phases, a phase diagram of the system at 1200 °C was drawn and is shown in Fig. 2. As is apparent from Fig. 2, $6Pr_2O_3\cdot V_2O_5$ is not stable but a new compound $3Pr_2O_3\cdot V_2O_5(Pr_3VO_7)$ was found. The compounds, $3La_2O_3\cdot V_2O_5$ and $3Nd_2O_3\cdot V_2O_5$ had been found in the La_2O_3-,[5] and Nd_2O_3-system[6] which have the same phase diagram pattern as that of the present system. $3Eu_2O_3\cdot V_2O_5$ was known to be stable[28] although it could not be found in the Eu_2O_3-V_2O_3-V_2O_5 system[8] at 1200 °C. An X-ray powder pattern of Pr_3VO_7 is similar to those of La_3VO_7 and Nd_3VO_7. The crystal system of the compounds has not been determined yet. The spacing and relative intensities of the compound were determined and are shown in Table 1.

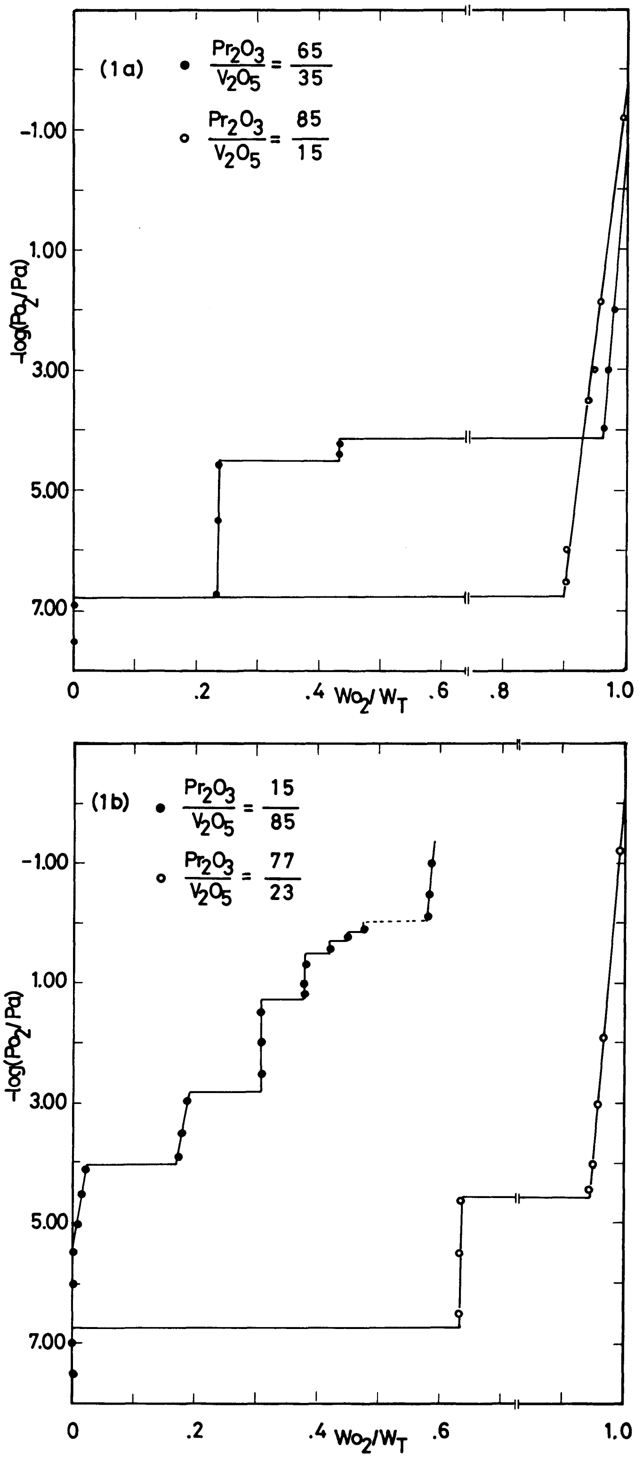

Fig. 1. The relationship between $-\log(P_{O_2}/\mathrm{Pa})$, and the composition, W_{O_2}/W_T, of samples. (1a) ●: $Pr_2O_3/V_2O_5=65/35$, ○: $Pr_2O_3/V_2O_5=85/15$, (1b) ●: $Pr_2O_3/V_2O_5=15/85$, ○: $Pr_2O_3/V_2O_5=77/23$.

Compound A might be $4Pr_2O_3\cdot V_2O_5$ reported by Brusset *et al.*[17] However, this compound does not have such a round mole ratio in the present case. This kind of compound has been found in La,[5] Nd,[6] Eu,[8] and Gd[4] systems, and will be found in a Tb system. It is interesting that these elements have a lower atomic number in the lanthanoid elements except for Sm in which system $5Sm_2O_3\cdot V_2O_5$ was stable at 1200 °C. Since $4Ln_2O_3\cdot V_2O_5$ was not detectable by our techniques, it might be nonstoichiometric toward the Ln_2O_3 side and mole ratio, $Ln_2O_3/V_2O_5=81/19$, might be rewritten to the ratio 4/1.

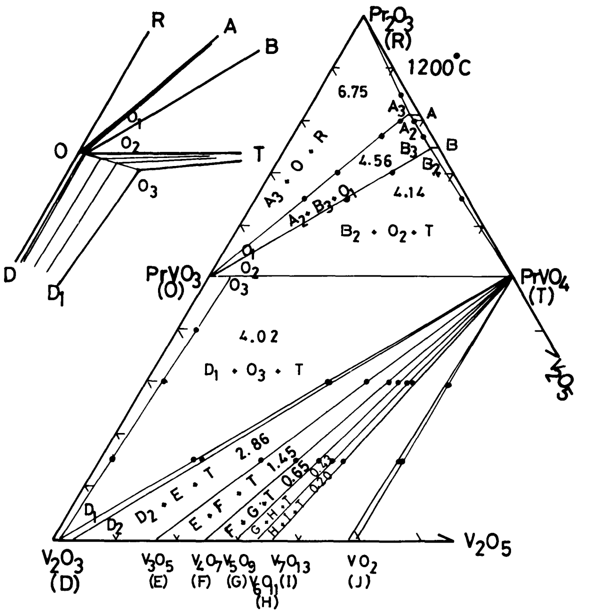

Fig. 2. Phase equilibria in the Pr_2O_3–V_2O_3–V_2O_5 system at 1200°C. Numerical values in the three-phase regions are the oxygen partial pressure in $-\log(P_{O_2}/Pa)$ in equilibrium. Symbols are the same as those in Table 3. A tentative, enlarged diagram near $PrVO_3$ was drawn on the left side with a little exaggeration.

Table 1. Spacings and relative intensities of $3Pr_2O_3 \cdot V_2O_5 (\log(P_{O_2}/Pa) = -4.30$, 47 h)

d/Å	I/I_0	d/Å	I/I_0
3.28	.83	2.161	.14
3.161	.74	1.983	.37
3.127	1.00	1.967	.29
3.056	.23	1.927	.26
3.014	.23	1.875	.23
2.933	.40	1.718	.17
2.808	.49	1.678	.14
2.719	.43		

Compounds A, Pr_3VO_7, $PrVO_4$, and $PrVO_3$ have nonstoichiometric compositions. The relationship between the composition and the oxygen partial pressure is represented by a linear equation, $N_O/N_A = a \log P_{O_2} + b$. Here, N_O is the mole fraction of the oxygen atom and N_A is the mole fraction of component A in the compound. The a and b values obtained from the results of the thermogravimetry are tabulated in Table 2. However, those values for $PrVO_4$ were not obtained because of the shortness of the solid-solution range.

Log $P_{O_2} = -4.14$ is the oxygen partial pressure in equilibrium with $Pr_3VO_7(B_2)$, $PrVO_4(T_1)$, and $PrVO_3(O_2)$, and on the other hand, log $P_{O_2} = -4.02$ is that in equilibrium with $V_2O_3(D_1)$, $PrVO_4(T_1)$, and $PrVO_3(O_3)$. This sort of the difference of the pattern was not found in the other systems reported by us. The solid-solution ranges for $PrVO_3$ with a mole ratio $Pr_2O_3/V_2O_5 \geqq 1$ and that for $PrVO_3$ with a mole ratio $Pr_2O_3/V_2O_5 < 1$ were apparently different. This phenomenum may be understood considering that $PrVO_3$ had a solid solution range toward the V_2O_3 and V_2O_5 side. A tentative phase diagram near $PrVO_3$ is depicted with a little exaggeration in the left side of Fig. 2.

Table 2. a and b values for the solid solutions ($N_O/N_X = a \log P_{O_2} + b$)

X	a	b
$PrVO_3$	0.0122	0.069
$0.81Pr_2O_3 \cdot 0.19V_2O_5$	4.00×10^{-3}	−0.018
$3Pr_2O_3 \cdot V_2O_5$	9.80×10^{-3}	−0.0124
$TbVO_4$	4.71×10^{-3}	2.07×10^{-3}
$0.81Tb_2O_3 \cdot 0.19V_2O_5$	7.00×10^{-3}	−0.015
$Y_8V_2O_{17}$	0.619	−0.124

Seven samples with Tb_2O_3/V_2O_5 mole ratio of 84/16, 8/2, 72/28, 65/35, 1, 3/7, and 15/85 were prepared to be used in thermogravimetric experiments. In Figs. 3a and 3b, the relationships between W_{O_2}/W_T and log (P_{O_2}/Pa) of samples, 84/16, 8/2, 72/28, and 15/85, are shown as representatives. Two oxygen partial pressures, 5.27 and 3.95 in $-\log P_{O_2}$, in equilibrium with three solid phases were obtained in addition to those in the V_2O_3–VO_2 subsystem. A phase diagram was depicted with the results of the thermogravimetry and the identification of phases and is shown in Fig. 4. The following phases are present; $Tb_2O_3(R')$, $0.81Tb_2O_3 \cdot 0.19V_2O_5(A')$, $TbVO_3$ (O′), and $TbVO_4(T')$ in addition to the compounds in the V_2O_3–VO_2 system.[1] The $5Tb_2O_3 \cdot V_2O_5$ was not stable. Using the quench method, the following two-phase combinations were confirmed; Tb_2O_3+A′, A′+$TbVO_4$, A′+$TbVO_3$, Tb_2O_3+$TbVO_4$, V_2O_3+$TbVO_3$, $TbVO_4$+V_nO_{2n-1} (n=2—7), and $TbVO_4$+VO_2. The pattern of Fig. 4 is similar to those of Eu_2O_3[8] and Gd_2O_3[4] systems which had been established.

Compounds A′ and $TbVO_4$ have nonstoichiometric compositions, but $TbVO_3$, on the other hand, is stoichiometric. a and b values for A′ and $TbVO_4$ are shown in Table 2 together with values for other compounds.

It has been confirmed that Y_2O_3 is stable under the present experimental conditions.[25] Seven samples with Y_2O_3/V_2O_5 mole ratios of 85/15, 8/2, 75/25, 65/35, 1, 25/75, and 1/9 were used for the establishment of the phase diagram in the thermogravimetry. The variation of the weight with log P_{O_2} for four samples, 85/15, 65/35, 1, and 1/9, were shown in Fig. 5 as representative cases. Two oxygen partial pressure, 4.62 and 3.98 in -log P_{O_2}, in equilibrium with three solid phases were found in addition to six values in the V_2O_3–VO_2 system. Compounds Y_2O_3(R″), $4Y_2O_3 \cdot V_2O_5$(A″), YVO_4(T″), and YVO_3-

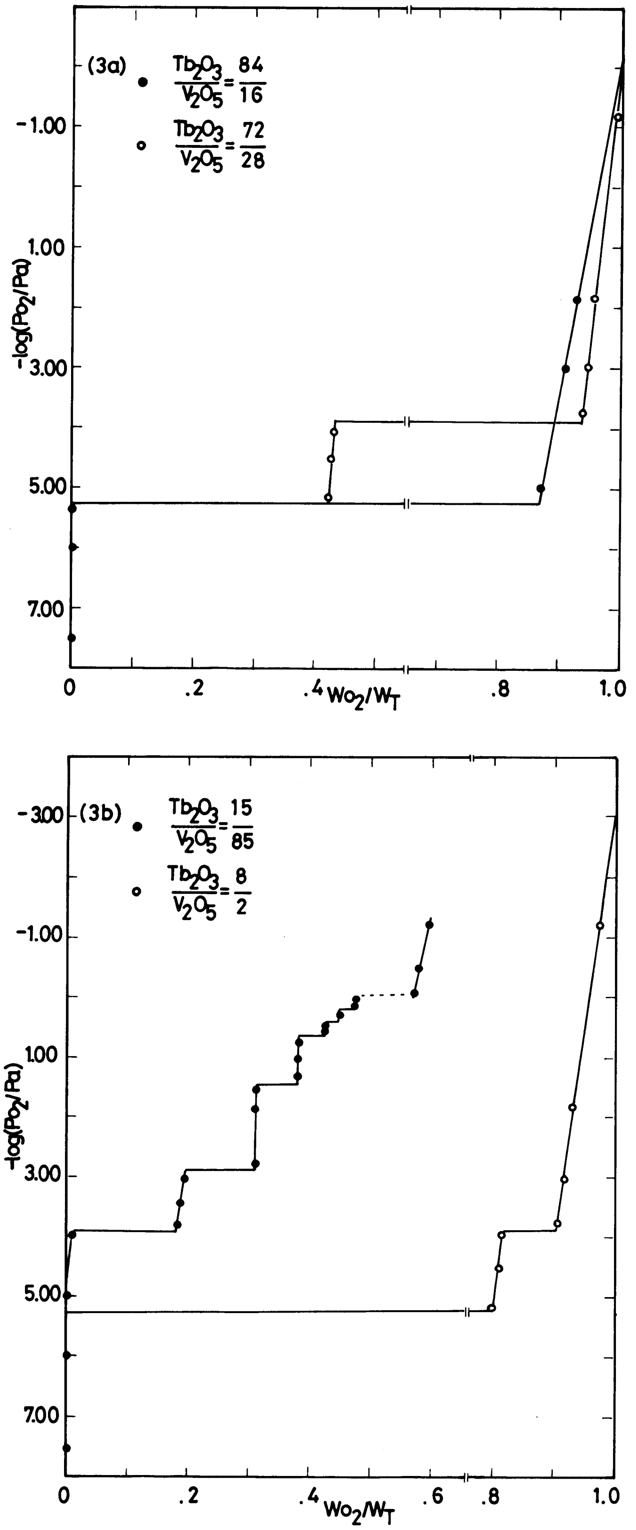

Fig. 3. The realtionship between $-\log(P_{O_2}/Pa)$ and the composition, W_{O_2}/W_T, of samples. (3a) ●: $Tb_2O_3/V_2O_5=84/16$, ○: $Tb_2O_3/V_2O_5=72/28$, (3b) ●: $Tb_2O_3/V_2O_5=15/85$, ○: $Tb_2O_3/V_2O_5=8/2$.

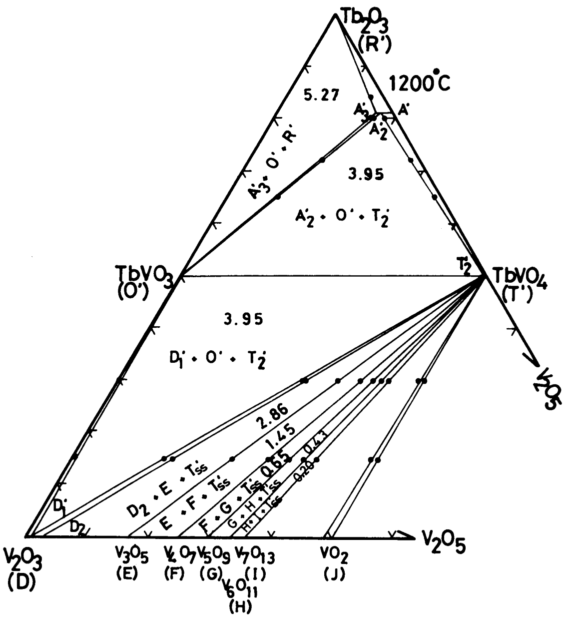

Fig. 4. Phase equilibria in the Tb_2O_3–V_2O_3–V_2O_5 system at 1200°C. Numerical values in the three-phase regions are the oxygen partial pressure in $-\log(P_{O_2}/Pa)$ in equilibrium. Symbols are the same as those in Table 3.

(O″) were confirmed to be stable by the quench method. Two-phase combinations are: Y_2O_3+A″, A″+YVO_4, A″+YVO_3, Y_2O_3+YVO_3, YVO_3+V_2O_3, YVO_4+V_{2n-1} (n=2—7), and VO_2+YVO_4. The $5Y_2O_3 \cdot V_2O_5$ was not found in the present system.

Compounds A″ and YVO_4 have nonstoichiometric compositions, and composition *vs.* $\log P_{O_2}$ for A″ is also tabulated in Table 2. The relation for YVO_4 could not determined because the non-stoichiomeric range is too narrow. Levin's report[16] regarding the pseudobinary of Y_2O_3–YVO_4 described above might imply the nonstoichiometry of $4Y_2O_3 \cdot V_2O_5$ and YVO_4.

Using the thermogravimetry results and the phase identification, a phase diagram at 1200 °C was drawn and is shown in Fig. 6. This diagram is a popular type and has one ternary compound, Ln_2O_3/V_2O_5= 4/1, in the Ln_2O_3–$LnVO_4$ subsystem. This diagram is similar to those of Dy_2O_3, Ho_2O_3, and Er_2O_3.

The activities of each components in a solid-solution were calculated using the Gibbs-Duhem equation and applying the relation between N_O/N_x and $\log P_{O_2}$ obtained above. The detailed method of the calculation has been discussed in a paper by Kimizuka and Katsura.[27] The results of the calculation are tabulated in Table 3 together with a composition of the compounds obtained by thermogravimetry, symbols of compounds, and the stability ranges of the compounds in terms of $\log P_{O_2}$. The activity of the $PrVO_3$ component at the composition O2 was chosen as unity. The activity of the $PrVO_3$ component at the composition O3 was not determined.

The lattice constants of the compounds A, A′, and A″ were successfully determined with the data of the assigment of $4Tm_2O_3 \cdot V_2O_5$[29] although errors were still large compared with the data of others. The values of the lattice constant of $LnVO_3$ and $LnVO_4$

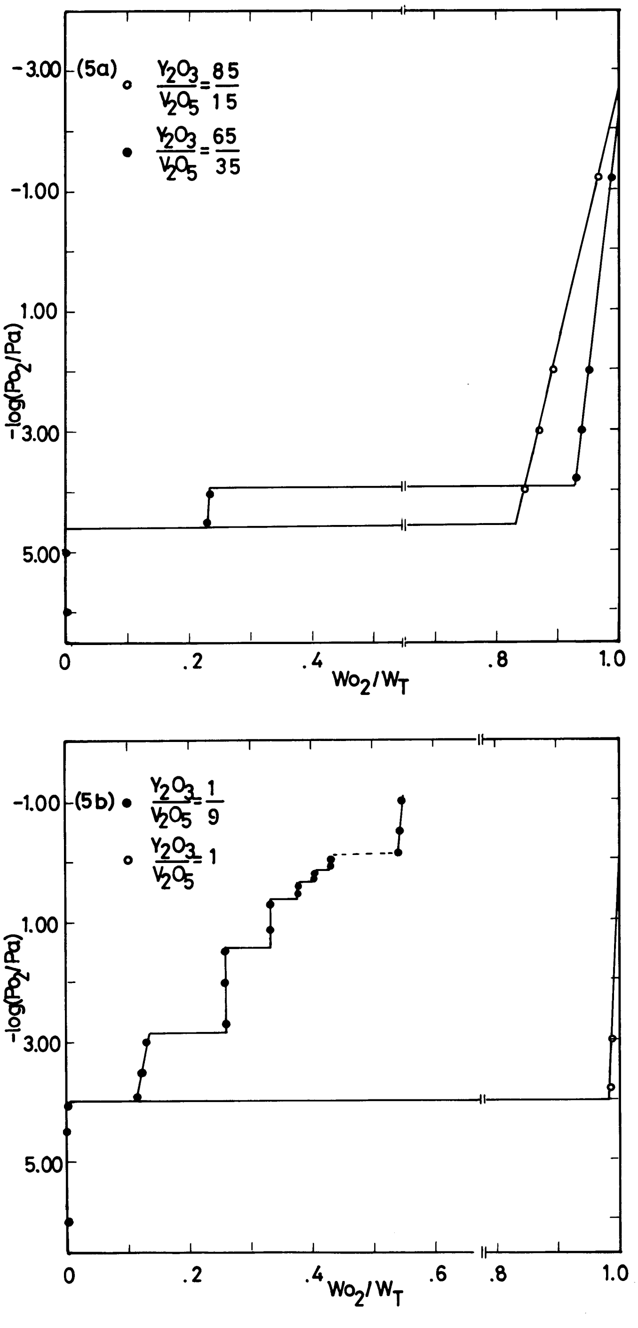

Fig. 5. The relationship between $-\log(P_{O_2}/\text{Pa})$ and the composition, W_{O_2}/W_T, of samples. (5a) ○: $Y_2O_3/V_2O_5=85/15$, ●: $Y_2O_3/V_2O_5=65/35$, (5b) ●: $Y_2O_3/V_2O_5=1/9$, ○: $Y_2O_3/V_2O_5=1$.

were also determined by the powder X-ray diffractometer and tabulated in Table 4 together with previous values. The ternary compounds which were made in the different conditions of the oxygen partial pressure show no considerable difference in lattice constant. Instrumental errors were calibrated by measuring the diffraction angles of a standard specimen of silicon.

Calculation of the Standard Gibbs Energies of Reactions.

On the basis of the established phase diagrams, the standard Gibbs energies of the reactions which are found in the phase diagrams can be calculated by the equation, $\Delta G°=-RT \ln K$, where the R is the gas constant, the T the absolute temperature, and the K the equilibrium constant of a reaction. Reactions and $\Delta G°$ values calculated are shown in Table 5 together with the oxygen partial pressures in equilibrium. The activities necessary for the calculation are shown in Table 3. The standard state can be arbitrarily chosen and, as described above, the activity of the $PrVO_3$ component at the composition O_2 was chosen as unity in this case. If the standard state are changed to that of the $PrVO_3$ component at the composition O_3, the $\Delta G°$ values for the reaction (3) is 127.2 kJ. The difference in $\Delta G°$ values is about 2 kJ.

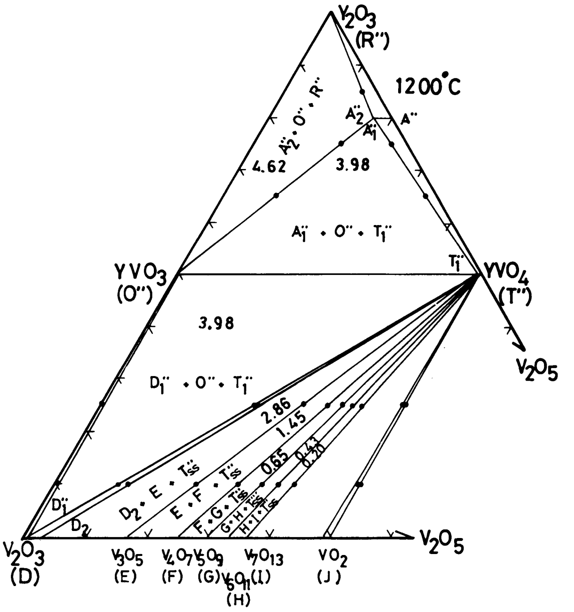

Fig. 6. Phase equilibria in the Y_2O_3-V_2O_3-V_2O_5 system at 1200 °C. Numerical values in the three-phase regions are the oxygen partial pressure in $-\log(P_{O_2}/\text{Pa})$ in equilibrium. Symbols are the same as those in Table 3.

The Relationship between ΔG° and Ionic Radius.

In a previous report,[7] the relationship between the $\Delta G°$ value for the reaction, $LnVO_3+1/2\ O_2=LnVO_4$, and the ionic radius of lanthanoid elements in 8 coordination had been shown graphically. According to the result, the lanthanoid group is divided into two groups and the relation is linear within each of groups. After the report[7] was published, the values for Eu, Yb, Dy, and Ho systems have also been confirmed to fit well to the previous linear relation. The present values are plotted in Fig. 7 with open circles together with solid circles of the previous data. The present values for Pr and Tb fit well to the previous line, but the value for Y is widely different from what was anticipated. The reason for this difference could not be elucidated. Perhaps it might be one of the reasons why Y has no property similar to lanthanoid contraction.

In the series of this study, a reaction, $3Ln_2O_3+2LnVO_3+O_2=4Ln_2O_3\cdot V_2O_5(Ln_8V_2O_{17})$, is often found although $0.81Ln_2O_3\cdot 0.19V_2O_5$ is stable instead of $4Ln_2O_3\cdot V_2O_5$ for La, Nd, Pr, Eu, Gd, and Tb. As described above, the composition $0.81Ln_2O_3\cdot 0.19V_2O_3$ is still unplausible and questionable, but the oxygen partial pressure in equilibrium with Ln_2O_3, $LnVO_3$, and $4Ln_2O_3\cdot V_2O_5$ or $0.81Ln_2O_3\cdot 0.19V_2O_5$ are valid within experimental errors. Thus, the relation be-

TABLE 3. COMPOSITIONS, SYMBOLS, STABILITY RANGES IN THE OXYGEN PARTIAL PRESSURES, AND ACTIVITIES OF THE SOLID SOLUTIONS

Component	Composition	Symbol	$-\log(P_{O_2}/Pa)$	$-\log a_i$
$Pr_{1.62}V_{0.38}O_{3.38}$	$Pr_{1.62}V_{0.38}O_{3.33}$	A_3	6.75	0
	$Pr_{1.62}V_{0.38}O_{3.34}$	A_2	4.56	0.045
	$Pr_{1.62}V_{0.38}O_{3.37}$	A_1	$-1.20(CO_2)$	0.116
Pr_3VO_7	$Pr_3VO_{6.94}$	B_3	4.56	0
	$Pr_3VO_{6.95}$	B_2	4.14	0.0116
	$Pr_3VO_{6.999}$	B_1	-1.20	0.0831
$PrVO_3$	$PrVO_{3.07}$	O_3	4.02	Not determined
	$PrVO_{3.02}$	O_2	4.14	0
	$PrVO_{3.01}$	O_1	4.56	3.35×10^{-3}
	$PrVO_{3.00}$	O	6.75—7.50[a)]	3.36×10^{-3}
$Tb_{1.62}V_{0.38}O_{3.38}$	$Tb_{1.62}V_{0.38}O_{3.33}$	A'_3	5.27	0
	$Tb_{1.62}V_{0.38}O_{3.34}$	A'_2	3.95	0.0318
	$Tb_{1.62}V_{0.38}O_{3.38}$	A'_1	-1.20	0.0951
$TbVO_3$	$TbVO_{3.00}$	O′	3.95—7.50[a)]	0
$TbVO_4$	$TbVO_{3.98}$	T'_2	3.95	0
	$TbVO_{4.00}$	T'_1	-1.20	0.0138
$Y_8V_2O_{17}$	$Y_8V_2O_{16.59}$	A''_2	4.62	0
	$Y_8V_2O_{16.65}$	A''_1	3.98	0.125
	$Y_8V_2O_{17.00}$	A″	-2.00—-4.32	0.679

a) This value is the lowest oxygen partial pressure in the present experiment. $PrVO_3$, $TbVO_3$, and YVO_3 may be stable in the lower oxygen partial pressure range than this value.

TABLE 4. UNIT CELL DIMENSIONS OF COMPOUNDS

Sample	$-\log(P_{O_2}/Pa)$	a/Å	b/Å	c/Å	β/°	V/Å³	Ref.
$PrVO_4$	-1.20	7.363±0.001		6.464±0.001		350.5±0.1	Present
	3.50	7.364±0.001		6.465±0.001		350.6±0.1	Present
		7.364±0.002		6.465±0.003			17)
$PrVO_3$	5.00[a)]	5.470±0.004	5.531±0.004	7.763±0.004		234.9±0.3	Present
	7.50	5.472±0.009	5.561±0.009	7.779±0.010		236.7±0.6	Present
		5.472±0.003	5.529±0.003	7.774±0.003		235.2±0.1	19)
		5.487	5.562	7.751			31)
A	-1.20	11.01±0.05	8.92 ±0.04	16.70±0.22	99.4±0.5	1618±24	Present
	6.50	11.01±0.06	8.91 ±0.05	16.67.±0.24	99.3±0.6	1615±25	Present
$TbVO_4$	-1.20	7.183±0.002		6.332±0.002		326.7±0.2	Present
		7.179±0.003		6.324±0.003			30)
$TbVO_3$	5.00	5.334±0.001	5.610±0.001	7.627±0.001		228.2±0.1	Present
		5.325±0.002	5.606±0.002	7.614±0.002		227.3±0.05	19)
A′	-1.20	10.71±0.04	8.45 ±0.06	15.80±0.11	97.9±0.3	1433±15	Present
	5.00	10.70±0.10	8.67 ±0.07	15.30±0.20	94.7±0.7	1410±28	Present
YVO_4	-4.32	7.115±0.012		6.327±0.013		320±1	Present
		7.119		6.290			16)
YVO_3	6.00	5.282±0.002	5.589±0.002	7.576±0.002		223.6±0.2	Present
		5.274±0.002	5.590±0.002	7.574±0.002		223.3±0.05	19)
		5.284	5.605	7.587			31)
A″	-4.32	10.52±0.06	8.32 ±0.03	15.78±0.13	97.6±0.5	1369±14	Present
	4.00	10.70±0.07	8.37 ±0.07	15.83±0.25	98.9±0.7	1402±27	Present

a) This sample, which has a starting mole ratio $Pr_2O_3/V_2O_5=4/6$, coexists with V_2O_3.

Table 5. The standard gibbs energies of reactions

	Reaction	$-\log(P_{O_2}/\mathrm{Pa})$	$-\Delta G^\circ/\mathrm{kJ}$
(1)	$31/50\mathrm{Pr_2O_3}+19/50\mathrm{PrVO_3}+19/100\mathrm{O_2}=\mathrm{Pr_{1.62}V_{0.38}O_{3.38}}$	6.75±0.08	62.9±1.0
(2)	$50/31\mathrm{Pr_{1.62}V_{0.38}O_{3.38}}+12/31\mathrm{PrVO_3}+6/31\mathrm{O_2}=\mathrm{Pr_3VO_7}$	4.56±0.05	50.1±0.5
(3)	$\mathrm{PrVO_3}+1/2\mathrm{O_2}=\mathrm{PrVO_4}$	4.14±0.03	128.9±0.5
(4)	$31/50\mathrm{Tb_2O_3}+19/50\mathrm{TbVO_3}+19/100\mathrm{O_2}=\mathrm{Tb_{1.62}V_{0.38}O_{3.38}}$	5.27±0.03	55.0±1.0
(5)	$\mathrm{TbVO_3}+1/2\mathrm{O_2}=\mathrm{TbVO_4}$	3.95±0.03	126.2±0.5
(6)	$3\mathrm{Y_2O_3}+2\mathrm{YVO_3}+\mathrm{O_2}=\mathrm{Y_8V_2O_{17}}$	4.62±0.02	271 ±1
(7)	$\mathrm{YVO_3}+1/2\mathrm{O_2}=\mathrm{YVO_4}$	3.98±0.02	126.6±0.5

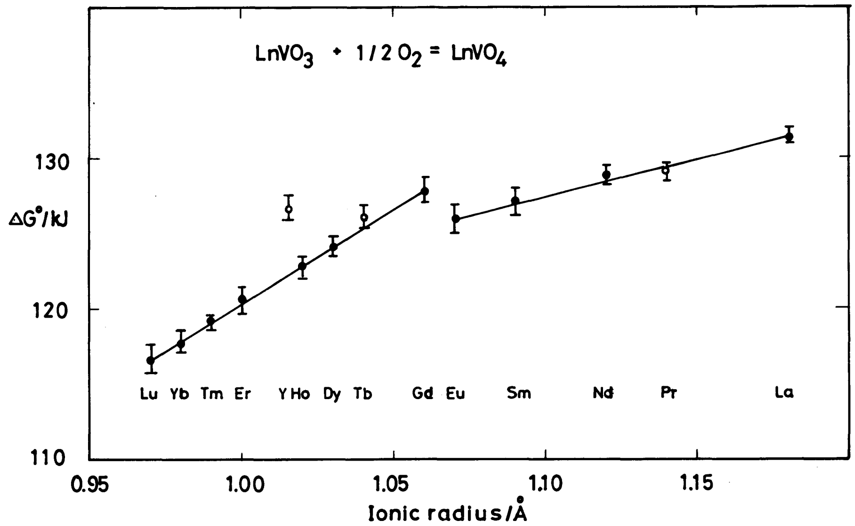

Fig. 7. The relationship between the ionic radius of lanthanoid elements in 8 coordination and the ΔG° values of reaction, $\mathrm{LnVO}+1/2\mathrm{O_2}=\mathrm{LnVO_4}$.

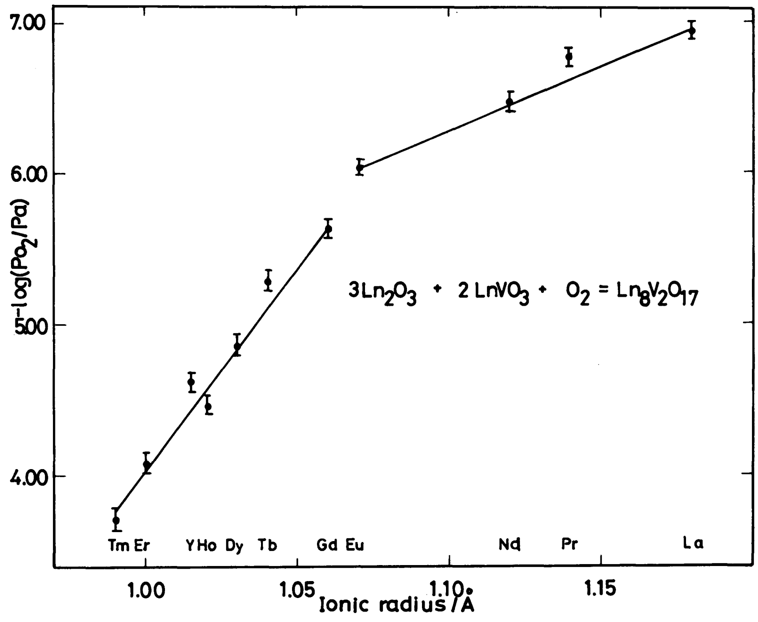

Fig. 8. The relationship between the ionic radius of lanthanoid elements in 8 coordination and the ΔG° values of reaction, $3\mathrm{Ln_2O_3}+2\mathrm{LnVO_3}+\mathrm{O_2}=\mathrm{Ln_8V_2O_{17}}$.

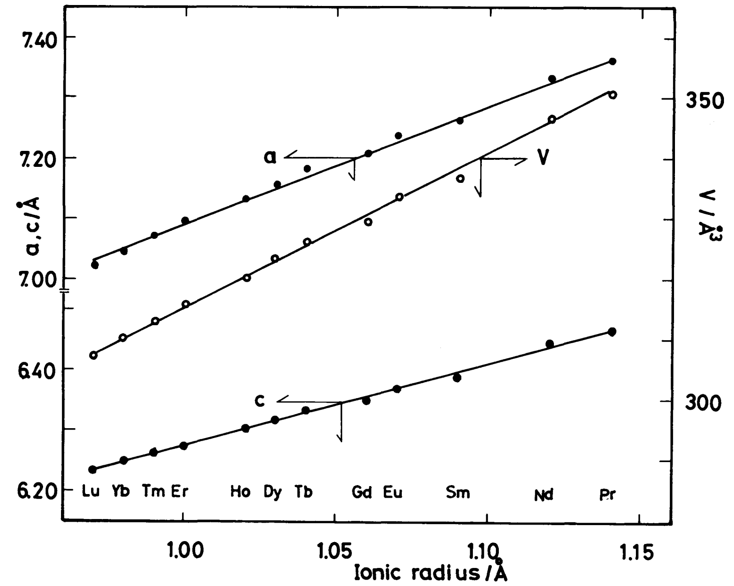

Fig. 9. Variations of the lattice parameter and the volume of $LnVO_4$ with Ln^{3+} radius (Å) in 8 coordination.

tween the oxygen partial pressure and the ionic radius of elements in the 8 coordination is plotted in Fig. 8. Comparing this with the previous case, the points are in a less linear fashion, but the same trend appears; that is, the lanthanoid elements are divided into two groups and in each group the relation is nearly linear.

Variations with Lattice Parameters with Ionic Radius. The lattice parameters and the volumes of $LnVO_4$ with a zircon structure are plotted as a function of the ionic radius in the 8 coordination in Fig. 9. Lattice parameters for other compounds have already been presented.[1–9] A smooth decreases in the *a*, *c*, and *V* values with atomic number is noted as would be expected from the lanthanoid contraction. The relation between lattice parameters and volumes of $LnVO_3$ and the ionic radius in 12 coordination is shown in Fig. 10. The *a*, *c*, and *V* values decrease with increasing atomic number and these values seem to form *a* gap at Gd. On the other hand, the *b* values show a gentle curve with a maximum near the intermeadiate atomic number. These characteristics were already pointed out by McCarthy *et al.*[19]

Classification of the Phase Diagram Pattern. According to a study of this series, systems at 1200 °C could be clssified into six groups with respect to the assemblages of ternary compounds. The La_2O_3–V_2O_3–V_2O_5 system belongs to the A-type in which three ternary compounds are stable in the Ln_2O_3–$LnVO_4$ subsystem, the (Pr and Nd)$_2O_3$–V_2O_3–V_2O_5 systems belong to the B-type in which two ternary compound, $0.81Ln_2O_3\cdot 0.19V_2O_5$ and Ln_3VO_7, are stable in the subsystem, the (Sm, Eu, Gd, Tb, Dy, Ho, and Er)$_2O_3$–V_2O_3–V_2O_5 systems belong to the C-type in which one ternary compound, $4Ln_2O_3\cdot V_2O_5$ or $0.81Ln_2O_3\cdot 0.19V_2O_5$ or $5Ln_2O_3\cdot V_2O_5$, is stable in the subsystem, the Tm_2O_3–V_2O_3–V_2O_5 system belongs to the D-type in which two ternary compounds, $4Tm_2O_3\cdot V_2O_5$ and $Tm_7V_3O_{16}$, are stable, the Yb_2O_3–V_2O_3–V_2O_5 system belongs to the E-type in which one compound $Yb_7V_3O_{16}$ is stable, and the Lu_2O_3–V_2O_3–V_2O_5 system belongs to the F-type in which three ternary compounds, $Lu_7V_3O_{16}$, $Lu_2V_2O_7$, and LuV_4O_8, are stable.

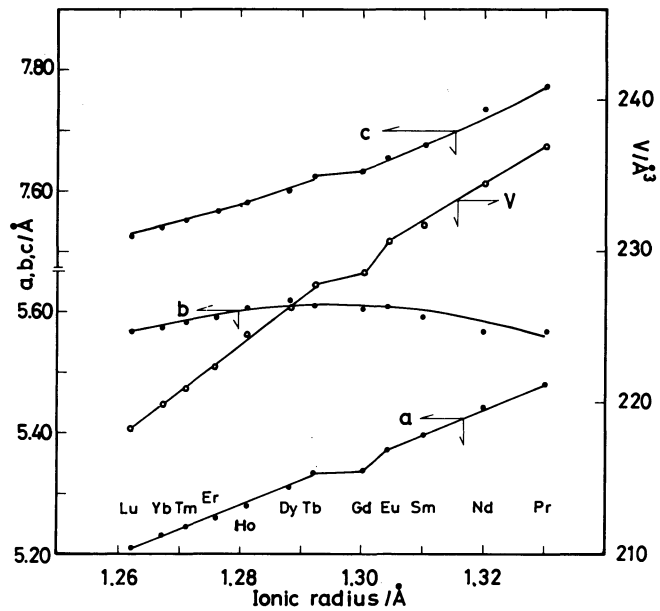

Fig. 10. Variations of the lattice parameter and the volume of $LnVO_3$ with Ln^{3+} radius (Å) in 12 coordination.

It would be interesting to know whether the ternary compound assemblages change or not upon changing the experimental temperature.

References

1) K. Kitayama and T. Katsura, *Bull. Chem. Soc. Jpn.*, **50**, 889 (1977).

2) K. Kitayama and T. Katsura, *Bull. Chem. Soc. Jpn.*, **51**, 1358 (1978).

3) K. Kitayama, T. Sugihara, and T. Katsura, *Bull. Chem. Soc. Jpn.*, **52**, 458 (1979).

4) K. Kitayama and T. Katsura, *Bull. Chem. Soc. Jpn.*, **55**, 1820 (1982).

5) K. Kitayama, D. Zoshima, and T. Katsura, *Bull. Chem. Soc. Jpn.*, **56**, 689 (1983).

6) K. Kitayama, C. Mizokuchi, and T. Katsura, *Bull. Chem. Soc. Jpn.*, **56**, 695 (1983).

7) K. Kitayama and T. Katsura, *Bull. Chem. Soc. Jpn.*, **56**, 1084 (1983).

8) K. Kitayama, H. Sou, and T. Katsura, *Bull. Chem. Soc. Jpn.*, **56**, 3415 (1983).

9) K. Kitayama and T. Katsura, *Bull. Chem. Soc. Jpn.*, **57**, 1222 (1984).

10) R. L. Martin, *Nature*, **165**, 202 (1950).

11) R. Ferguson, E. D. Guth, and L. Eyring, *J. Am. Chem. Soc.*, **76**, 3890 (1954).

12) R. P. Turcotte, J. M. Warmkessel, R. J. D. Tilley, and L. Eyring, *J. Solid State Chem.*, **3**, 265 (1971).

13) E. D. Guth and L. Eyring, *J. Am. Chem. Soc.*, **76**, 5242 (1954).

14) N. C. Baenziger, H. A. Eick, H. Schulett, and L. Eyring, *J. Am. Chem. Soc.*, **83**, 2219 (1961).

15) T. Sugihara, Theses, Tokyo Institute of Technology 1978.

16) E. M. Levin, *J. Am. Ceram. Soc.* **50**, 381 (1967).

17) H. Brusset, F. Madaule-Aubry, B. Blanck, J. P. Glaziou, and J. P. Laude, *Can. J. Chem.*, **49**, 3700 (1971).

18) T. Shinike, G. Adachi, and J. Shiokawa, *Nippon Kagaku Kaishi*, **1974**, 1038.

19) G. J. McCarthy, C. A. Sipe, and K. E. McIlvried, *Mat. Res. Bull.*, **9**, 1279 (1974).

20) T. Shinike, G. Adachi, and J. Shiokawa, *Denki Kagaku*, **48**, 258 (1980).

21) J.C.P.D.S. Card, No. 6-410.

22) J.C.P.D.S. Card, No. 23-1418.

23) T. Katsura and H. Hasegawa, *Bull. Chem. Soc. Jpn.*, **40**, 561 (1967).

24) T. Katsura and A. Muan, *Trans. AIME*, **230**, 77 (1964).

25) N. Kimizuka and T. Katsura, *J. Solid State Chem.*, **13**, 176 (1975).

26) N. Kimizuka and T. Katsura, *J. Solid State Chem.*, **15**, 151 (1975).

27) N. Kimizuka and T. Katsura, *Bull. Chem. Soc. Jpn.*, **47**, 1801 (1974).

28) S. S. Kiparisov, R. A. Belyaev, V. V. Bondarenko, and V. P. Vyskubov, *Izv. Akad. Nauk SSSR, Neorg. Mat.*, **9**, 68 (1973).

29) H. Brusset, R. Mahe, and J. P. Laude, *Bull. Soc. Chim. Fr.*, 495 (1973).

30) H. Schwartz, *Z. Anorg. Allgem. Chem.*, **323**, 44 (1963).

31) B. Reuter, *Col. Inst. C.N.R.S.*, 1053 (1965).

32) J.C.P.D.S. Card, No. 17-341.